Defective monocyte enzymatic function and an inhibitory immune phenotype in HIV-exposed uninfected African infants in the era of antiretroviral therapy

Louise Afran[1,2,3], Kondwani C. Jambo[1,3], Wilfred Nedi[1], David JC Miles[1,4], Anmol Kiran[1, 7], Dominic H Banda[1], Ralph Kamg'ona[1], Dumizulu Tembo[1], Annette Pachnio[4], Eleni Nastouli[6], Brigit Ferne[6], Henry C Mwandumba[1,3], Paul Moss[4], David Goldblatt[6], Sarah Rowland-Jones[5], Adam Finn[1], Robert S Heyderman[1, 6]

[1] Malawi-Liverpool-Wellcome Trust Clinical Research Programme, University of Malawi College of Medicine, Blantyre, Malawi, [2]Bristol Children's Vaccine Centre, Schools of Cellular & Molecular Medicine and of Population Health Sciences, University of Bristol, Bristol, United Kingdom, [3]Department of Clinical Sciences, Liverpool School of Tropical Medicine, Liverpool, United Kingdom, [4] University of Birmingham, Birmingham, United Kingdom, [5]University of Oxford, Nuffield Department of Medicine, Oxford, United Kingdom, and [6]University College London, Division of Infection and Immunity, London, United Kingdom, and [7]University of Edinburgh, Edinburgh, United Kingdom.

Correspondence to: *Louise Afran, Malawi-Liverpool-Wellcome Trust Clinical Research Programme, P.O Box 30096, Chichiri, Blantyre 3, Malawi. Email: Lafran@mlw.mw Tel: +0992118817

There were no conflicts of interest. This work was funded by the Wellcome trust and the Franklin Adams trust.

Running title: Immune dysregulation in HEU African infants

Summary: Early life HIV-exposure may dysregulate innate and adaptive immunity, specifically, monocyte function and vaccine induced immunity to encapsulated bacteria. This may lead to altered protection and susceptibility to disease from encapsulated bacteria.

Keywords. HIV-exposure, immune dysregulation, monocyte function, neonatal vaccine immunity, HIV-1, ART, Human herpes virus,

Abstract

Background. HIV-Exposed Uninfected (HEU) infants are a rapidly expanding population in sub-Saharan Africa, highly susceptible to encapsulated bacterial disease in the first year of life. The mechanism of this increased risk is still poorly understood. We investigated if HIV-exposure dysregulates HEU immunity, vaccine-antibody production and human herpes virus (HHV) amplify this effect.

Methods. 34 HIV-infected and 44 HIV-uninfected pregnant women were recruited into the birth cohort, followed up to 6 weeks of age; and 43 HIV-infected and 61 HIV-uninfected mother-infant pairs into a longitudinal infant cohort, at either: 5-7 to 14-15; or 14-15 to 18-23 weeks of age. We compared monocyte function, innate and adaptive immune cell phenotype, and vaccine-induced antibody responses between HEU and HU infants.

Results. We demonstrate altered monocyte phagosomal function and B cell subset homeostasis, and lower vaccine-induced anti-*Haemophilus influenzae type b* (*Hib)* and anti-Tetanus Toxoid (TT) IgG titers in HEU compared to HU infants. HHV infection was similar between HEU and HU infants.

Conclusion. In the era of antiretroviral therapy (ART)-mediated viral suppression, HIV-exposure may dysregulate monocyte and B cell function, during the vulnerable period of immune maturation. This may contribute to the high rates of invasive bacterial disease and pneumonia in HEU infants.

Keywords. HIV-exposure; neonates; infants; innate immunity; adaptive immunity; vaccines; CMV; EBV.

Introduction

HIV-exposed uninfected (HEU) infants are particularly vulnerable to invasive bacterial disease[1,2] particularly, pneumonia[3] and diarrhea[4], they have more frequent hospitalisations, more severe infections and increased risk of treatment failure. However, the mechanism of this increased vulnerability remains unknown. The global population of HEU children is substantial, estimated at 1.2 million births annually, mainly within developing countries[8]. Therefore, a coordinated strategy is necessary to ensure their optimal health and wellbeing[9].

The vulnerability of HEU infants is likely a complex intersection of HIV-exposure immune profile 'remodelling', 'inflammatory' maternal cytokine milieu[10], time of antiretroviral therapy (ART) initiation[11], ART use[12] and prophylactics [13], increased exposure to maternal viral/bacterial pathogens, and host microbial/environmental factors. Pre-vaccination antibody levels are lower in HEU infants, but normalise to HU infants levels post-vaccination [5–7]. Together these result in a more permissive state for the development of infections [1]. Many observational studies reported immunological abnormalities in HEU infants [14] including highly differentiated T-cells [15] and B-cell subsets [16], altered responses to vaccines [17], functional impairment of natural killer cells [18] and monocytes [19]. Furthermore, few studies considered early transmission of immunomodulatory human herpes virus' (HHVs), cytomegalovirus (CMV)[20]/Epstein Barr virus (EBV)[21] recrudescence during pregnancy, as HHVs are important drivers of inflammation in HEU infants[20].

Due to the successful HIV test and treat strategy globally, the prevalence of individuals receiving ART has risen considerably[8]. Consequently, the number of HEU infants born to mothers receiving ART increased markedly, but despite expanded implementation of prevention of vertical transmission programmes, the risk of infection-related morbidity and mortality among HEU infants remains high[2], particularly the risk of encapsulated bacterial infection[22]. The immune profile amongst HEU infants is

not well documented. We therefore, addressed whether HIV-exposure and HHVs dysregulate infant immunity and/or the response to primary vaccination.

Methods

Study Design and population. The study was conducted in Southern Malawi, at Ndirande Health Centre (NHC) (primary healthcare facility in Blantyre) and at Queen Elizabeth Central Hospital (QECH) (tertiary teaching hospital in Blantyre). We recruited HEU and HU infant cohorts in two contiguous groups that were followed longitudinally pre- and post-routine childhood vaccination with pentavalent DPT-HepB-Hib immunisation. The first group were aged 5-9 weeks (pre-1st vaccine dose), who were followed upto age 14-15 weeks (post-2nd vaccine dose) and the second group were aged 14-15 weeks (post-2nd vaccine dose) who were followed upto 18-23 weeks of age (post-3rd vaccine dose). We also recruited pregnant women in the early stages of labour at QECH maternity ward and subsequently their babies at birth (termed new born birth cohort). Participating mothers were healthy(without disease), asymptomatic adults (≥18 yr) comprising HIV-infected and HIV-uninfected volunteers. HIV testing was performed on maternal whole blood in the early stages of labour or at recruitment using two commercial point-of-care rapid HIV test kits, Determine HIV 1/2 kit (Abbott Diagnostic Division, Abbott Park, IL) and Unigold HIV 1/2 kit (Trinity Biotech Inc., Bray, Ireland) and had a CD4+ T-cell count performed. HIV-infected participants received first line ART (Option B+ (Lamivudine, Tenofovir DF and Efavirenz (3TC/TDF/EFV)) during or pre-pregnancy. All HEU babies received nevirapine at birth for 6 weeks, followed by co-trimoxazole until 1 year of life. Exclusion criteria for the study participants were current or past history of smoking, heart disease, tuberculosis, high blood pressure, drug use, syphilis, severe anaemia (haemoglobin <8 g/dl), placental abnormalities, infant prematurity, low birth weight or death and existing comorbidities. All babies received Bacille Calmette Guerin (BCG) vaccine at birth. Written informed consent was obtained from all participants prior to recruitment. Ethical approval was obtained

from the University of Malawi College of Medicine Research and ethics committee (COMREC), Blantyre, Malawi, protocol numbers P.11/11/1140, P.06/11/1088.

Sample collection and processing. We collected 5ml of venous blood from the infants, at 5-9, 14-15 and 18-23 weeks of age following attendance at the vaccination clinic for pentavalent DPT-HepB-Hib immunisation. Participants with incomplete vaccine course were excluded. Mothers had 10ml of venous blood collected at the first visit and 3mls of breastmilk at all other time points. We collected upto 40ml cord blood from the umbilical vein into sodium heparinised tubes using a 50ml syringe, from the new born interface of the placenta immediately after birth. Whole blood was kept at room temperature and processed within 2 hours. Peripheral blood mononuclear cells were isolated by density centrifugation. Plasma was separated by centrifugation at 1500rpm for 10 minutes, aspirated, aliquoted and stored at -80 for later use. Breastmilk samples were collected by hand expression, fractionated into lipid and aqueous phase and stored at -80. Due to limitations in the volume of blood collectable from very young babies and limited cell numbers, not all the assays were performed on every new born or infant sample.

HIV testing. New borns and infants qualitative HIVDNA PCR tests were performed in batches of 23 at MLW core labs. Total DNA was isolated from 0.5 $x10^6$ cells using AMPLICOR HIV-1 DNA test, V1.5 (Roche, USA) according to the manufacturer's instructions. HIV DNA results in participant health passports were also collected.

Three HIV-RDT kits, from two separate manufacturers (Unigold™ and Determine™) were used to confirm the presence or absence of HIV specific immunoglobulins (Ig) in maternal peripheral blood. Cord blood mononuclear cells were stored in 500ul of RNAlater and analysed at UCL by digital PCR as described elsewhere [23].

Maternal CD4 counts. Peripheral blood CD4 T-counts and full blood count were performed at the Malawi-Liverpool Wellcome Trust Clinical Research Programme Diagnostic Laboratory on an Hmx

analyser (Beckman Coulter, USA) using a standardized protocol. Blood was taken in the early stages of labour.

Phenotypic analysis. Multicolour flow cytometry analysis was performed on whole blood. Samples were stained with the following fluorochrome conjugated antibodies, anti-CD14 Phyocoerythrin Cyanine-7 (PECy7), anti-CD3 Allophycocyanin-H7 (APC-H7), anti-CD4 Pacific Blue (PB), anti-CD8 Fluorescein (FITC), anti-CD8 (PECY7), CD45RA Phyocoerythrin (PE), CD45RA PECY5, CCR7 Allophycocyanin (APC), anti-CD19 (APC), anti-CD19 Peridinin-Chlorophyll-Protein (PERCP), anti-CD27 (PE), , CD10 PE-Cy7, CD21 FITC, CD27 APC-Cy7, CD95 e450, FcLR4 PE, CD57 FITC, PD-1 APC, PD-1 PE (Supplementary 2-5 Gating strategy and Table 2). Samples were acquired on Beckman Coulter Cyan ADP and analyses were performed using FlowJo Version 7.6.5 and 10.5 software (Treestar).

Measurement of monocyte phagosomal enzymatic activity. Phagosomal oxidative burst and bulk proteolytic function in monocytes was measured using a flow cytometry–based reporter bead assay as described previously [24], (supplementary methods 1a).

T cell IFNγ ELISpot. 2x10^6 PBMCs were stimulated with GAG peptides in an 18-hour IFN-γ T cell ELISpot as previously described [25], (supplementary methods 1b).

Human cytomegalovirus PCR . Real time PCR was used to detect hCMV in HIV-infected and uninfected maternal breast milk and infant oropharangeal throat swabs (supplementary methods 1c).

Detection of Cytomegalovirus specific IgG and IgM antibodies. hCMV specific IgM in HIV-infected and uninfected maternal and infant plasma was measured using a commercial ELISA kit (IBL International, Hamburg) according to manufacturer's instructions. A semi-quantitative, in-house hCMV IgG assay was used at the laboratories in the University of Birmingham, UK, (supplementary methods 1d).

Epstein-Barr virus nested PCR

A nested PCR measuring EBNA3B gene in HIV-infected and uninfected maternal breast milk and infant throat swabs were used (method as described in [26]).

Detection of Epstein Barr Virus specific IgG antibodies

IgG antibodies against EBV viral capsid antigen (VCA) were detected in plasma using a commercial Enzyme Linked Immunosorbent Assay kit (ELISA) (Diagnostic Automation, California) according to manufacturer's instructions.

Sandwich enzyme-linked immunosorbent assay to detect IgG specific to vaccine antigens. In an in-house ELISA, TT or DT (both NIBSC, UK) (supplementary methods 1e). Optical density was measured (without acid stopping the reaction) after 10 min using an ELISA plate reader (Biotek, UK) set at 405nm and SoftMax Pro software.

Multiplexed opsonophagocytosis killing assay and serotype-specific IgG . Immunoglobulin G (IgG) serum concentrations specific for the 13 pneumococcal vaccine serotypes (1, 3, 4, 5, 6 A, 6B, 7F, 9V, 14, 18C, 19A, 19F, and 23F) were measured using an enzyme-linked immunosorbent assay (ELISA), described in supplementary methods 1f.

Statistical analysis. Statistical analysis and graphical presentation were performed using Prism 7/8 (GraphPad Software, San Diego, USA) and Python (Python Software Foundation) was used to calculate summary statistics. Demographic and clinical characteristics were compared using Mann-Whitney-U for continuous and Fisher's exact tests or χ^2 for discrete variables. ELISpot data were reported as subtracted 2 x background. Serotype-specific opsonophagocytic indexes (OPIs) were reported using geometric means and 95% confidence intervals. The OPIs were classified as being positive or negative based on the

current recommended cut-off value of <8 (negative) and ≥8 (positive). Results are reported as median and IQR as stated.

Results

Participant characteristics

In the new born birth cohort, 34 HIV-infected and 44 HIV-uninfected pregnant women were recruited, two new borns were excluded from the analysis due to death and HIV-positivity detected by digital droplet PCR. HIV-infected pregnant women received ART Option B+ (tenofovir/lamivudine/efavirenz) for an average of 18.7 (range 1-143) months, with a mean nadir CD4+ T-cell count of 294 (range 8-892) and were more likely to have had an elective caesarean birth, compared to HIV-uninfected pregnant women(p=0.01). In the longitudinal infant cohort, 43 HIV-infected and 61 HIV-uninfected mother-infant pairs were recruited and sampled across time points, 5-9, 14-15, 18-23 weeks of age, corresponding to the Malawian routine infant vaccine schedule of: BCG at birth, then pentavalent vaccine at 6, 10, 14 weeks. HIV-infected women had received option B+ for an average of 9.28 (range 1-72) months at the time of enrollment and had a mean nadir CD4+ T-cell count of 409 (range 159-823). There was no difference between maternal age or breastfeeding status but mode of delivery was more often caesarean section in HIV-infected mothers compared to HIV-negative mothers (Table 1).

Defective monocyte enzymatic function

Firstly, we used a flow cytometry-based whole blood phagocyte functional reporter bead assay[24] to assess monocyte function in cord blood from the birth cohort (Figure 1a; Supplementary Figure 1). We assessed the ability of monocytes to internalise Alexa Fluor 405-labeled IgG-coated reporter beads at 1 hour post co-incubation, as a proxy of uptake capacity. We showed that the proportion of monocytes that internalised reporter beads was similar between HEU infants and HU controls (56[43-64] Vs. 70[31-

76] p=0.86) (Figure 1b), (HU, n=16; HEU, n=12).We next assessed the phagosomal superoxide burst activity, and found that it was lower in monocytes from HEU infants compared to HU controls (1[0.8-1.6] Vs. 3.9[2.7-8.9], p=0.0001)(Figure 1c). Third, we assessed the phagosomal bulk proteolytic activity and showed that it was lower in monocytes from HEU new borns compared to HU controls (1.3[0.94-2.2] Vs. 2.8[2.1-3.3], p=0.0025) (Figure 1d). Collectively, these data indicate altered monocyte phagosomal functional capacity at birth in HEU new borns.

Increased B-cell inhibitory phenotype and PPD responses but decreased T-cell PHA responses

We next sought to investigate dysregulation in the adaptive arm of immunity using cord blood. We observed similar distributions of B cell subsets between HEU and HU new born babies p>0.1, including, $CD10^-CD21^+CD27^-$ (naive), $CD10^-CD21^-CD27^+$ (resting memory), $CD10^-CD21^+CD27^+$ (activated memory), $CD10^-CD21^-CD27^-$ (tissue-like memory) and $CD10^+CD27^-$ (immature transitional) B cells (Figure 2a), (HU, n=42; HEU, n=18). However, we found a higher proportion (%) of Fc-receptor like 4 ($FcRL4^+$) expressing B cells in HEU new borns (3.11 [0.82-6] Vs. 0.7 [0.44-1.5] , p=0.0004), but no statistically significant differences in the proportion of PD-1 (3.3 [2-6.9] Vs. 2.1 [1.3-5], p=0.09) or CD95-expressing B cells (0.38 [0.17-0.44] Vs. 0.15 [0.05-0.31], p=0.1), when compared to HU controls (Figure 2b). $FcLR4^+$ inhibits B cell activation through the B cell receptor (BCR) and is a marker of B cell exhaustion in chronically HIV-infected adults, which suggests increased B cell regulation in HEU new born babies.

Next, using peripheral blood collected from the longitudinal infant cohort aged 5-9 weeks, we also found B cell alterations in two subsets that are selectively dysregulated during chronic HIV infection [27,28]. The proportions of immature transitional and tissue-like memory B cells were lower in HEU infants than HU controls (7.6 [1.2-16] Vs. 12 [6.4-21] p=0.04)(Supplementary Figure 2a); but the proportions of naive and central memory, $CD4^+$ and $CD8^+$ T cell subsets were similar, p>0.1,(Supplementary Figure 2b-c).

When we looked at T cells from cord blood, the proportion of naive and central memory CD4+ and CD8+ T cell subsets measured by CD45RA, CCR7 expression were similar between HEU new borns and HU controls, p>0.5 and p>0.1, respectively, (Figure 3a-b) (HU, n=41; HEU, n=24).. As were the proportion of CD57 or PD-1-expressing $CD4^+$ (p=0.08, p=0.79) and $CD8^+$ T cells (p=0.38, p=0.22) respectively, (Figure 3c). Morever, mean IFNγ production in response to tuberculin purified protein derivative (PPD) in an 18-hour ELISpot assay was similar in HEU new borns compared to controls (1[1-62] Vs. 1[1-58] [min-max], p=0.13), (HU, n=35; HEU, n=21). In this population BCG is received soon after birth. However, IFNγ production in response to the selective T cell mitogen phytohemagglutinin (PHA) was reduced in HEU new borns compared to controls (64 [1-141] Vs. 165[6.6-299], p=0.03) (figure 3d), indicating selective regulation of T-cell responses. We then evaluated PBMCs from infant peripheral blood, for IFNγ spot forming cells (SFCs) to tetanus toxoid (TT), hepatitis B (Hb) and purified protein derivative (PPD) in an 18-hour T-cell ELIspot. We observed increased IFNγ SFCs/million PBMCs to PPD amongst HEU infants, compared to HU controls (143 [42-268] Vs. 34 [3.3-79]p=0.03), but similar Hb (p=0.78), TT (p=0.26) and PHA (p=0.75) responses (Supplementary figure 2d). These data indicate that antigen-specific responses to PPD in HEU infants following BCG vaccination are enhanced.

Decreased vaccine-induced anti-Heamophilus influenzae type b and diphtheria toxoid titres but preserved opsonophagocytosis activity to PCV13 serotypes

Using peripheral blood from infants, we next interrogated vaccine-induced memory B cell antibody responses to polysaccharide and protein antigens that are in the Malawian infant primary vaccination series; including PCV13 (HU,n=11; HEU,n=9) and Pentavalent Vaccine (DPT-HepB-Hib) (HU, n=50; HEU n=39), 14-15 (HU, n=22; HEU, n=27) and 18-23 (HU, n=25; HEU, n=19).

Following 3 vaccine doses, we found lower GMT(SD) anti-*Hib* (0.67(3.7) Vs. 1.8 (3.4), p=0.014) and anti-diphtheria toxoid (DT) titers (1.6(7.4) Vs. 4.1(2.2), p=0.036), but similar anti-TT titers (0.47(0.4) Vs.

0.57(0.28), p=0.27) in HEU infants, compared to HU controls (Figure 4a and Supplementary figure 6a-b). In the mothers of these infants, anti-*Hib* IgG (0.52 (2.5)Vs. 0.99 (2.8), p=0.0015) and anti-TT (0.13 (2.3) Vs. 0.21(2.4), p=0.002) IgG titres but not anti-DT titers (0.05(4.62) Vs. 0.05(3.5), p=0.91) were lower in HIV-infected mothers than HIV-uninfected controls (Figure 4b-c and Supplementary figure 6c).

We next tested whether HIV-exposure influences the levels of vaccine-induced functional antibody in infants aged 5-9 weeks. Using a Multiplex Opsonophagocytosis Assay, we measured opsonophagocytic activity of 13 vaccine serotypes from the PCV13 (1, 3, 4, 5, 6A, 6B, 7F, 9V, 14, 18C, 19A, 19F, 23F) in infant sera. We found no difference in the geometric mean opsonophagocytic index of 13 pneumococcal serotypes and geometric mean concentration (GMC) of serotype-specific IgG titres, between HEU infants and HU controls (Table 2).

To determine potential drivers of the described immune alterations in new borns and infants, we measured HIV Gag-specific responses in cord and peripheral blood mononuclear cells [29] using an 18-hour *ex-vivo* IFN-γ ELISpot assay in both the HEU new born and the longitudinal infant cohorts, (Figure 5a-b; Supplementary Figure 7a) (HU, n =22; HEU, n=34; HIV+ART+, n=17; HIV+ART-, n=8) and (HU, n =35; HEU, n=23), respectively. Few Gag-specific responses were detectable in cord blood of HEU new borns (p=0.05) (Supplementary Figure 7a). However, in older infants there was detectable IFN-γ producing HIV Gag-specific cell responses in approximately 50% of the longitudinal cohort of HEU infants (mean 22 (50%) Vs. 4.3 (18%),p=0.01)(Figure 5b).

We then assessed the association of EBV/CMV exposure as a potential driver of immune alterations.We found that anti-hCMV IgG titers were higher in plasma from HEU infants aged 5-15 weeks, than HU controls (86% Vs. 79.8%, p=0.012) (Figure 5c) (HU, n =57; HEU, n=42), but hCMV PCR detection in throat swabs was similar using a chi-square test (29% Vs. 14%, p=0.19)(Supplementary Figure 8a) (HU, n =19; HEU n=33), indicating potential differences in the pattern of exposure to hCMV. In maternal breastmilk,

we found a higher proportion of hCMV PCR positive HIV-infected mothers compared to HIV-uninfected controls (31(89%) Vs. 13(57%), p=0.005)(Figure 5d) (HIV-, n =57; HIV+ n=42).

EBV sero-positivity is rapid upto one year of life [21]. In our infant cohort EBV viral capsid antigen detection by anti-IgG (p=0.07) was high in plasma but PCR detection was low (p=0.22) in throat swabs, EBV results were not significantly different between HEU and HU groups (Supplementary Figure 8b-c) (HU, n =24; HEU n=34). Taken together, HHV (hCMV and EBV) infection are common in infancy in this setting, irrespective of HIV-exposure status.

Discussion

HIV-exposed but uninfected infants are at an increased risk of infectious disease even in the era of universal access to maternal ART, however, the underlying immunological basis is not well understood. We show altered monocyte phagosomal function, dysregulated B cell homeostasis and selective impairment of vaccine responses in HEU infants within the first 6 months of life. We also demonstrate evidence of HIV-exposure and increased likelihood of hCMV exposure in HEU infants. We postulate that the variable severity and/or persistence of this immunological phenotype may explain the variable clinical manifestations reported in HEU infants [30,31], which may depend on the duration and intensity of exposure to HIV and other infectious co-factors.

The impaired monocyte phagosomal function in HEU new borns highlights their potential vulnerability to bacterial infection before the primary immunisation series. Monocyte bactericidal activity requires uptake, reactive oxygen species (ROS) formation and phagosomes-lysosomes fusion resulting in inhibition, killing and degradation of internalised bacteria [32]. In our setting, the validated flow cytometer reporter assay of phagocyte function which uses zymosan, has shown poor immune function and superoxide burst activity in HIV-infected adults with active tuberculosis (TB)[33]. Monocyte functional impairment against encapsulated bacteria has also been observed in “age-associated”

inflammation, where monocyte-activating cytokines TNF-α and IL-6 are augmented [34]. Similarly, increased monocyte inflammatory markers, including sTNF-RI, IL-6, IP-10, oxLDL and sCD14 are reported in HEU new borns [32]; as well as enhanced pro-inflammatory cytokine secretion following stimulation with diverse PAMPs at 6 weeks of age [35]. Moreover, recent PBMC transcriptomic profiling in HEU infants aged 1-2 years, revealed down-regulated genes (LCN2, CAMP, HP, MMP8, BPI, LTF) associated with neutrophil function[36]. Taken together this may explain HEU infant increased susceptibility to bacterial infection and pneumonia.

We also found increased FcLR4 expression on B-cells. In chronically HIV-infected adults, the inhibitory B cell receptor FcLR4 are over-represented, an 'exhausted' B cell phenotype, with poor B cell receptor mediated activation and antigen-specific antibody production [37,38]. In HEU infants at 6 to 14 weeks of age, we observed low proportions of tissue-like memory and immature-transitional B-cell subsets, which conversely, are augmented in chronically HIV-infected adults [39,40] and are indicative of dysregulated B cell homeostasis. Importantly, our data presents evidence of increased exposure to HIV and hCMV in HEU infants from maternal HIV and/or viral proteins, hCMV recrudescence and high PPD specific IFNγ, that may promote B cell dysregulation in early life. PPD responses are shown to be increased in *Mycobacterium tuberculosis* (Mtb) sensitised mothers, [41] and a bimodal response to BCG/PPD (high/low) has been reported in HEU infants in our setting[42]; BCG vaccination induces heterologous effects in myeloid cells at an epigenetic level in a process termed 'trained immunty'[43], which may explain our findings. Taken together, the mechanisms of B cell dysregulation are likely distinct from those seen in chronic HIV infection (hypergammaglobulinaemia), due to the lack of replicative virus and preserved CD4 T-cells.

Altered B cell homeostasis is associated with impaired antibody responses during chronic HIV infection [44,45]. Consistent with this observation, HIV-infected mothers in our cohort exhibited lower anti-Hib and anti-TT antibody titers than HIV-uninfected mothers using the Pentavalent Vaccine (DPT-HepB-Hib).

In agreement with maternal titers, we observed low anti-Hib titers in HEU infants. However, our observation is in contrast with studies conducted in South Africa [46] and Uganda [47,48], who reported robust anti-Hib and anti-DT antibody titers in HEU infants. Differential vaccine immunogenicity is likely multifactorial, influenced by persistent immune exposure to HIV proteins, the time to maternal ART use and the unique burden of infectious co-factors that likely contribute to a microenvironment of pro-inflammation. Consistent with previous observations [49], we also observed that a relatively large number of HEU infants mounted an IFN-γ response following stimulation with HIV Gag, however we did not detect IFN-γ responses in HEU new borns, and responses were poor to the T cell mitogen PHA (which crosslinks the TCR/glycosylated surface proteins). Taken together, these data point towards HIV-exposure as a possible driver of selective T cell regulation at birth.

Our study limitations, include: the limited no. of assays per sample restricted adjustment for multiple comparisons; we exclused premature/low-birth weight/small for gestational age babies; no maternal viral load or clinical presentation of disease were taken; and HIV-negative mothers were not retested at the study end.

In conclusion, we show altered monocyte phagosomal function, dysregulated B cell homeostasis and selective impairment of vaccine antibody responses in HEU infants within the first 6 months of life. This period of vulnerability likely contributes to increased susceptibility to disease-causing bacteria that commonly cause life-threating illness such as pneumonia in HEU infants.

Financial support. This work was supported by the Wellcome trust and a studentship from the Franklin Adams trust. The Malawi-Liverpool-Wellcome Trust Clinical Research Programme was supported by a strategic award from the Wellcome Trust. RSH is a NIHR Senior Investigator. The views expressed are those of the author(s) and not necessarily those of the NIHR or the UK Government Department of Health and Social Care.

Acknowledgments

The authors are grateful to the participants for their willingness to participate in this study.

Author contribution

L.A. A.F, R.S.H, S.R.J, D.M contributed to study design. L.A, A.B, B.F, R.K, D.H.B, D.G, P.M, D.M performed the experiments. W.N recruited and monitored the participants. L.A, K.C.J analysis and interpretation. H.M, D.M, A.F., K.C.J, R.S.H, reviewed the manuscript.

Potential conflicts of interest. All authors: No reported conflicts of interest.

References

1. Afran L, Garcia Knight M, Nduati E, Urban BC, Heyderman RS, Rowland-Jones SL. HIV-exposed uninfected children: a growing population with a vulnerable immune system? Clin Exp Immunol [Internet]. **2014** [cited 2014 Mar 10]; 176(1):11–22. Available from: http://doi.wiley.com/10.1111/cei.12251

2. Roux SM le, Abrams EJ, Donald KA, et al. Infectious morbidity of breastfed, HIV-exposed uninfected infants under conditions of universal antiretroviral therapy in South Africa: a prospective cohort study. Lancet Child Adolesc Heal. Elsevier B.V.; **2020**; 4(3):220–231.

3. Adler C, Haelterman E, Barlow P, Marchant A, Levy J, Goetghebuer T. Severe Infections in HIV-Exposed Uninfected Infants Born in a European Country. Davies M-A, editor. PLoS One [Internet]. **2015** [cited 2015 Nov 25]; 10(8):e0135375. Available from: http://www.pubmedcentral.nih.gov/articlerender.fcgi?artid=4540431&tool=pmcentrez&rendertype=abstract

4. Andersson AK, Sumariwalla PF, McCann FE, et al. Blockade of NKG2D ameliorates disease in mice with collagen-induced arthritis: A potential pathogenic role in chronic inflammatory arthritis. Arthritis Rheum [Internet]. **2011** [cited 2019 Jun 24]; 63(9):2617–2629. Available from: http://doi.wiley.com/10.1002/art.30460

5. Jones CE. Maternal HIV Infection and Antibody Responses Against Vaccine-Preventable Diseases in Uninfected Infants. JAMA [Internet]. **2011**; 305(6):576. Available from: http://jama.ama-assn.org/content/305/6/576.abstract

6. Baroncelli S, Galluzzo CM, Liotta G, et al. Dynamics of immunoglobulin G subclasses during the first two years of life in Malawian infants born to HIV-positive mothers. BMC Pediatr [Internet]. BioMed Central Ltd.; **2020** [cited 2020 Sep 4]; 20(1). Available from: https://pubmed.ncbi.nlm.nih.gov/32326903/

7. Succi RCM, Krauss MR, Harris DR, et al. Immunity after Childhood Vaccinations in Perinatally HIV-exposed Children with and Without HIV Infection in Latin America. Pediatr Infect Dis J. Lippincott Williams and Wilkins; **2018**; 37(4):304–309.

8. UNAIDS. Joint United Nations Programme on HIV/AIDS [Internet]. 2019 [cited 2020 Dec 31]. Available from: https://www.unaids.org/en/resources/documents/2019/2019-UNAIDS-data

9. South A, Slogrove L, Johnson F, et al. Estimates of the global population of children who are HIV-exposed and uninfected, 2000-18: a modelling study. Artic Lancet Glob Heal [Internet]. **2020** [cited 2020 Aug 22]; 8:67–75. Available from: http://aidsinfo.unaids.org

10. Sevenoaks T, Wedderburn CJ, Donald KA, et al. Association of maternal and infant inflammation with neurodevelopment in HIV-exposed uninfected children in a South African birth cohort. Brain Behav Immun [Internet]. **2020** [cited 2020 Sep 4]; . Available from: http://www.ncbi.nlm.nih.gov/pubmed/32860940

11. Goetghebuer T, Smolen KK, Adler C, et al. Initiation of Antiretroviral Therapy Before Pregnancy Reduces the Risk of Infection-related Hospitalization in Human Immunodeficiency Virus-exposed Uninfected Infants Born in a High-income Country. Clin Infect Dis [Internet]. Oxford University Press; **2019** [cited 2020 Sep 9]; 68(7):1193–1203. Available from: https://pubmed.ncbi.nlm.nih.gov/30215689/

12. Dyke RB Van, Chadwick EG, Hazra R, Williams PL, Seage GR. The PHACS SMARTT Study: Assessment of the Safety of In Utero Exposure to Antiretroviral Drugs. Front Immunol [Internet]. Frontiers Media S.A.; **2016** [cited 2020 Dec 31]; 7(MAY):23. Available from: http://journal.frontiersin.org/Article/10.3389/fimmu.2016.00199/abstract

13. D'Souza AW, Moodley-Govender E, Berla B, et al. Cotrimoxazole prophylaxis increases resistance gene prevalence and α-diversity but decreases β-diversity in the gut microbiome of HIV-exposed, uninfected infants. Clin Infect Dis [Internet]. Oxford University Press (OUP); **2019** [cited 2020 Sep 4]; . Available from: http://www.ncbi.nlm.nih.gov/pubmed/31832638

14. Goetghebuer T, Rowland-Jones SL, Kollmann TR. Editorial: Immune Mechanisms Underlying the Increased Morbidity and Mortality of HIV-Exposed Uninfected (HEU) Children. Front Immunol [Internet]. **2017** [cited 2017 Oct 23]; 8:1060. Available from: http://journal.frontiersin.org/article/10.3389/fimmu.2017.01060/full

15. Jalbert E, Williamson KM, Kroehl ME, et al. HIV-exposed uninfected infants have increased regulatory T cells that correlate with decreased T cell function. Front Immunol. Frontiers Media S.A.; **2019**; 10(MAR).

16. Nduati EW, Nkumama IN, Gambo FK, et al. HIV-Exposed Uninfected Infants Show Robust Memory B-Cell Responses in Spite of a Delayed Accumulation of Memory B Cells: an Observational Study in the First 2 Years of Life. Staats HF, editor. Clin Vaccine Immunol [Internet]. **2016** [cited 2017

Oct 23]; 23(7):576–85. Available from: http://cvi.asm.org/lookup/doi/10.1128/CVI.00149-16

17. Mazzola NBMA. Vaccines Response in HIV-Exposed Uninfected Infants. Clin vaccine Immunol. **2011**; (July).

18. Gasper MA, Kunwar P, Itaya G, et al. Natural killer cell and T-cell subset distributions and activation influence susceptibility to perinatal HIV-1 infection. AIDS [Internet]. **2014** [cited 2014 Oct 28]; 28(8):1115–24. Available from: http://www.ncbi.nlm.nih.gov/pubmed/24752082

19. Reikie BA, Adams RCM, Leligdowicz A, et al. Altered innate immune development in HIV-exposed uninfected infants. J Acquir Immune Defic Syndr [Internet]. Lippincott Williams and Wilkins; **2014** [cited 2020 Sep 16]; 66(3):245–255. Available from: /pmc/articles/PMC4146715/?report=abstract

20. Garcia-Knight MA, Nduati E, Hassan AS, et al. Cytomegalovirus viraemia is associated with poor growth and T-cell activation with an increased burden in HIV-exposed uninfected infants. AIDS [Internet]. Lippincott Williams and Wilkins; **2017** [cited 2020 Dec 31]; 31(13):1809–1818. Available from: https://pubmed.ncbi.nlm.nih.gov/28609400/

21. Montoya-Ferrer A, Sanosyan A, Fayd'herbe de Maudave A, et al. Clinical and Biological Factors Associated With Early Epstein-Barr Virus Infection in Human Immunodeficiency Virus–Exposed Uninfected Infants in Eastern Uganda. Clin Infect Dis [Internet]. Oxford University Press (OUP); **2020** [cited 2020 Dec 31]; . Available from: https://pubmed.ncbi.nlm.nih.gov/32067040/

22. Cools P, Wijgert JHHM van de, Jespers V, et al. Role of HIV exposure and infection in relation to neonatal GBS disease and rectovaginal GBS carriage: a systematic review and meta-analysis. Sci Rep [Internet]. Nature Publishing Group; **2017** [cited 2019 Sep 11]; 7(1):13820. Available from: http://www.ncbi.nlm.nih.gov/pubmed/29062060

23. Busby E, Whale AS, Ferns RB, et al. Instability of 8E5 calibration standard revealed by digital PCR risks inaccurate quantification of HIV DNA in clinical samples by qPCR. Sci Rep [Internet]. Nature Publishing Group; **2017** [cited 2018 Apr 13]; 7(1):1209. Available from: http://www.nature.com/articles/s41598-017-01221-5

24. Jambo KC, Banda DH, Kankwatira AM, et al. Small alveolar macrophages are infected preferentially by HIV and exhibit impaired phagocytic function. Mucosal Immunol [Internet]. **2014** [cited 2014 Mar 20]; . Available from: http://www.ncbi.nlm.nih.gov/pubmed/24472847

25. Kabilan L, G A, F L, HP E, T O, M. T-B. Detection of intracellular expression and secretion of

interferon-gamma at the single-cell level after activation of human T cells with tetanus toxoid in vitro. Eur J Immunol. **1990**; 20(5):1085–9.

26. Wakefield AJ, Fox JD, Sawyerr AM, et al. Detection of herpesvirus DNA in the large intestine of patients with ulcerative colitis and Crohn's disease using the nested polymerase chain reaction. J Med Virol [Internet]. **1992** [cited 2018 Dec 17]; 38(3):183–90. Available from: http://www.ncbi.nlm.nih.gov/pubmed/1287131

27. Sciaranghella G, Tong N, Mahan AE, Suscovich TJ, Alter G. Decoupling activation and exhaustion of B cells in spontaneous controllers of HIV infection. AIDS [Internet]. **2013** [cited 2014 May 8]; 27(2):175–80. Available from: http://www.pubmedcentral.nih.gov/articlerender.fcgi?artid=3729211&tool=pmcentrez&rendertype=abstract

28. Ho J, Moir S, Malaspina A, et al. Two overrepresented B cell populations in HIV-infected individuals undergo apoptosis by different mechanisms. Proc Natl Acad Sci U S A [Internet]. **2006** [cited 2015 Feb 9]; 103(51):19436–41. Available from: http://www.pubmedcentral.nih.gov/articlerender.fcgi?artid=1748244&tool=pmcentrez&rendertype=abstract

29. Cox JH, Ferrari G, Janetzki S. Measurement of cytokine release at the single cell level using the ELISPOT assay. Methods [Internet]. Methods; **2006** [cited 2020 Sep 8]; 38(4):274–282. Available from: https://pubmed.ncbi.nlm.nih.gov/16473524/

30. Musimbi ZD, Rono MK, Otieno JR, et al. Peripheral blood mononuclear cell transcriptomes reveal an over-representation of down-regulated genes associated with immunity in HIV-exposed uninfected infants. Sci Rep. Nature Research; **2019**; 9(1).

31. Dauby N, Chamekh M, Melin P, Slogrove AL, Goetghebuer T. Increased Risk of Group BStreptococcusInvasive Infection in HIV-Exposed but Uninfected Infants: A Review of the Evidence and Possible Mechanisms. Front Immunol [Internet]. Frontiers Media SA; **2016** [cited 2018 Feb 16]; 7(NOV):505. Available from: http://www.ncbi.nlm.nih.gov/pubmed/27899925

32. Amer AO, Swanson MS. A phagosome of one's own: A microbial guide to life in the macrophage [Internet]. Curr. Opin. Microbiol. Elsevier Ltd; 2002 [cited 2020 Sep 16]. p. 56–61. Available from: https://pubmed.ncbi.nlm.nih.gov/11834370/

33. Gupta-Wright A, Tembo D, Jambo KC, et al. Functional Analysis of Phagocyte Activity in Whole

Blood from HIV/Tuberculosis-Infected Individuals Using a Novel Flow Cytometry-Based Assay. Front Immunol [Internet]. Frontiers; **2017** [cited 2019 Jun 6]; 8:1222. Available from: http://journal.frontiersin.org/article/10.3389/fimmu.2017.01222/full

34. Puchta A, Naidoo A, Verschoor CP, et al. TNF Drives Monocyte Dysfunction with Age and Results in Impaired Anti-pneumococcal Immunity. Philpott DJ, editor. PLOS Pathog [Internet]. Public Library of Science; **2016** [cited 2020 Sep 17]; 12(1):e1005368. Available from: https://dx.plos.org/10.1371/journal.ppat.1005368

35. Reikie BA, Adams RCM, Leligdowicz A, et al. Altered innate immune development in HIV-exposed uninfected infants. J Acquir Immune Defic Syndr [Internet]. **2014** [cited 2015 Dec 15]; 66(3):245–55. Available from: http://www.ncbi.nlm.nih.gov/pubmed/24732876

36. Musimbi ZD, Rono MK, Otieno JR, et al. Peripheral blood mononuclear cell transcriptomes reveal an over-representation of down-regulated genes associated with immunity in HIV-exposed uninfected infants. Sci Rep [Internet]. Nature Research; **2019** [cited 2020 Dec 31]; 9(1). Available from: https://pubmed.ncbi.nlm.nih.gov/31792230/

37. Kardava L, Moir S, Wang W, et al. Attenuation of HIV-associated human B cell exhaustion by siRNA downregulation of inhibitory receptors. J Clin Invest [Internet]. The American Society for Clinical Investigation; **2011**; 121(7):2614–2624. Available from: http://www.jci.org/articles/view/45685

38. Moir S, Fauci AS. Insights Into B Cells And Hiv-Specific B-Cell Responses In Hiv-Infected Individuals. Immunol Rev. **2013**; 254(1):207–224.

39. Malaspina A, Moir S, Ho J, et al. Appearance of immature/transitional B cells in HIV-infected individuals with advanced disease: Correlation with increased IL-7. Proc Natl Acad Sci U S A [Internet]. **2006** [cited 2015 Feb 9]; 103(7):2262–2267. Available from: https://www.pnas.org/content/103/7/2262.short

40. Malaspina A, Moir S, Chaitt DGD, et al. Idiopathic CD4+ T lymphocytopenia is associated with increases in immature/transitional B cells and serum levels of IL-7. Blood [Internet]. **2007** [cited 2020 Sep 14]; 109(5):2086–2088. Available from: https://ashpublications.org/blood/article-abstract/109/5/2086/23260

41. Jones CE, Hesseling AC, Tena-Coki NG, et al. The impact of HIV exposure and maternal Mycobacterium tuberculosis infection on infant immune responses to bacille Calmette-Guérin

vaccination. AIDS. Lippincott Williams and Wilkins; **2015**; 29(2):155–165.

42. Miles DJC, Gadama L, Gumbi A, Nyalo F, Makanani B, Heyderman RS. Human immunodeficiency virus (HIV) infection during pregnancy induces CD4 T-cell differentiation and modulates responses to Bacille Calmette-Guérin (BCG) vaccine in HIV-uninfected infants. Immunology [Internet]. Blackwell Publishing Ltd; **2010** [cited 2014 Mar 13]; 129(3):446–454. Available from: http://doi.wiley.com/10.1111/j.1365-2567.2009.03186.x

43. Netea MG, Joosten LAB, Latz E, et al. Trained immunity: A program of innate immune memory in health and disease [Internet]. Science (80-.). American Association for the Advancement of Science; 2016 [cited 2021 Mar 4]. p. 427. Available from: https://pubmed.ncbi.nlm.nih.gov/27102489/

44. Ray JE, Dobbs KR, Ogolla SO, et al. Reduced Transplacental Transfer of Antimalarial Antibodies in Kenyan HIV-Exposed Uninfected Infants. Open forum Infect Dis [Internet]. Oxford University Press; **2019** [cited 2020 Sep 4]; 6(6):ofz237. Available from: http://www.ncbi.nlm.nih.gov/pubmed/31214627

45. Dzanibe S, Adrian P V., Kimaro Mlacha SZ, Dangor Z, Kwatra G, Madhi SA. Reduced transplacental transfer of group b streptococcus surface protein antibodies in HIV-infected mother-newborn dyads. J Infect Dis [Internet]. Oxford University Press; **2017** [cited 2020 Sep 4]; 215(3):415–419. Available from: https://pubmed.ncbi.nlm.nih.gov/27932617/

46. Jones CE, Naidoo S, Beer C De, Esser M, Kampmann B, Hesseling AC. Maternal HIV Infection and Antibody Responses Against Vaccine-Preventable Diseases in Uninfected Infants. JAMA [Internet]. **2011** [cited 2019 Jul 10]; 305(6):576. Available from: http://jama.ama-assn.org/content/305/6/576.abstract

47. Simani OE, Izu A, Nunes MC, et al. Effect of HIV exposure and timing of antiretroviral therapy initiation on immune memory responses to diphtheria, tetanus, whole cell pertussis and hepatitis B vaccines. Expert Rev Vaccines. Taylor and Francis Ltd; **2019**; 18(1):95–104.

48. Gaensbauer JT, Rakhola JT, Onyango-Makumbi C, et al. Impaired haemophilus influenzae type b transplacental antibody transmission and declining antibody avidity through the first year of life represent potential vulnerabilities for HIV-exposed but -uninfected infants. Clin Vaccine Immunol [Internet]. **2014** [cited 2019 Jul 10]; 21(12):1661–7. Available from: http://www.ncbi.nlm.nih.gov/pubmed/25298109

49. Legrand FA, Nixon DF, Loo CP, et al. Strong HIV-1-Specific T Cell Responses in HIV-1-Exposed Uninfected Infants and Neonates Revealed after Regulatory T Cell Removal. Unutmaz D, editor. PLoS One [Internet]. Public Library of Science; **2006** [cited 2014 Feb 14]; 1(1):e102. Available from: http://www.ncbi.nlm.nih.gov/pubmed/17183635

50. WHO. Weekly epidemiological record Relevé épidémiologique hebdomadaire [Internet]. 2006. Available from: http://www.who.int/wer

Tables

Table 1. Participant characteristics among HEU new borns, infants and HU controls

	n=44	n=34		n=61	n=43	
	New born Birth cohort			**Longitudinal Infant cohort**		
Maternal status	HIV-	HIV+	*p-value*	HIV-	HIV+	*p-value*
[a]Mothers age in years median (IQR)	27.6 (23.6-32.95)	29.7(25.95-32.2)	0.86	21.9 (19.5-26.2)	28.8 (25.2-33.1)	0.37
[a]Mothers ART no.(%)	N/A	34/34 (100)	-	N/A	37/43 (86)	-
[a]Mothers time on ART months mean (range)	N/A	18.17 (1-143)	-	N/A	9.28 (0-72)	-
[a]Mothers time on ART pre-pregnancy count(%)	N/A	16/34(47)		N/A	10/43 (23)	
[a]Mothers time on ART 1st trimester count(%)	N/A	0/34(0)		N/A	1/43(2)	
[a]Mothers time on ART 2nd trimester count(%)	N/A	9/34(26)		N/A	5/43(12)	
[a]Mothers time on ART 3rd trimester count(%)	N/A	9/34(26)		N/A	15/43(35)	
[a]Mothers who did not receive ART during pregnancy, count(%)	N/A	0/34(0)		N/A	12/43(28)	
[a]Mothers CD4+ cells µL mean (range)	N/A	294 (8-892)	N/A	N/A	409 (159-823)* *	-
[a]Mothers no. caesarean Section (%)	0/44 (0)	14/34 (39)	**0.01**	-	-	-
No. mothers self-reported exclusive	44/44 (100)	34/34 (100)	**-**	61/61	43/43	-

breastfeeding (%)						
	HU new born	HEU new born	*p-value*	HU infant	HEU infant	*p-value*
[a]Female Sex of child (%)	22/44	15/34	0.65	29/61 (55)	22/43 (39)	0.24
No. who tested negative for HIV DNA PCR at birth (%)	-	31/34 (100)		-	43/43	-
No. who tested negative for HIV DNA PCR at 6 wks (%)	-	34/34 (100)		-	36/43 (83.7)*	-

Abbreviations: IQR, interquartile range; No., number; %=percentage; µL= microliter; dPCR=digital PCR, RDT = rapid diagnostic test performed on whole blood. [a] Calculated using Mann-Whitney for continuous variables or Fishers exact test for categorical variables. *7/43 unconfirmed HIV status, **3 mothers had missing CD4 data. Median(IQR) and mean(range) are reported.

HIV-infected participants received first line ART (Option B+ (Lamivudine, Tenofovir DF and Efavirenz (3TC/TDF/EFV)) at any point during pregnancy and had a CD4+ T-cell count performed. New borns and infants were tested with a HIV DNA PCR test at birth and 6 weeks as part of the early infant diagnosis programme in Malawi, new borns were additionally tested by digital droplet HIV DNA PCR at UCL labs. Mothers self reported exclusive breast feeding at the time of recruitment, which was birth, 6 weeks and 14 weeks..

Table 2. Robust opsonising and killing function of anti-pneumococcal capsular polysaccharide specific IgG antibodies in infant serum

	n=11	n=9		n=11	n=8	
PCV13 Serotypes	**HU infants GMOI (95% CI)**	**HEU infants GMOI (95% CI)**	***p-value***	**HU infants GMC (95% CI)**	**HEU infants GMC (95% CI)**	***p-value***
4	52.70 (12.02 – 231.1)	69.57 (8.32 – 581.9)	0.95	0.52 (0.19-1.42)	0.9 (0.2-4.03)	0.66

6B	39.97 (7.27 – 219.6)	65.58 (5.72 – 752.1)	0.76	0.39 (0.2-0.76)	0.55 (0.17-1.83)	0.75
14	169 (37.31 – 765.2)	223 (32.02 - 1553)	0.82	0.46 (0.2-1.08)	0.84 (0.21-3.3)	0.48
23F	48.82 (10.19 – 233.9)	78.70 (7.61 – 813.5)	0.80	0.38 (0.18-0.79)	0.51 (0.15-1.77)	0.99
6A	46.37 (5.9 – 364.3)	74.07 (5.68 – 966.9)	0.72	0.29 (0.16-0.52)	0.51 (0.15-1.8)	0.32
9V	65.79 (11.18 – 387.1)	82.85 (9.02 – 761.2)	0.93	0.4 (0.17-0.91)	0.74 (0.19-2.9)	0.42
18C	55.35 (11.88 - 258)	70.12 (8.6 – 570.9)	0.80	0.71 (0.24-2.07)	1.17 (0.18-7.48)	0.99
19F	74.04 (14.81-370.2)	92.55 (11.48-746)	0.93	0.65 (0.3-1.42)	1.08 (0.31-3.81)	0.49
1	11.22 (6.65-18.92)	16.39 (6.35-42.26)	0.49	2.19 (0.96-5.02)	2.5 (0.65-9.74)	0.82
5	17.79 (6.98-45.31)	26.98 (7.97-91.28)	0.44	0.53 (0.23-1.21)	0.62 (0.136-2.84)	0.83
7F	142.4 (25.17-805.4)	117.4 (10.02-1376)	0.87	0.63 (0.21-1.86)	1.20 (0.19-7.50)	0.66
19A	23.52 (6.64-83.31)	47.49 (5.76-391.3)	0.63	1.11 (0.33-3.72)	2.31 (0.4-13.37)	0.50
3	22.37 (8.4-59.54)	24.31 (6.58-89.82)	0.90	0.32 (0.15-0.7)	0.56 (0.2-1.63)	0.48

Abbreviations: GMOI (geometric mean opsonophagocytic index), GMC (geometric mean concentration) 95% CI (95% confidence interval), PCV13 (pneumococcal conjugate vaccine 13) The geometric mean opsonic index (GMOI) and 95% confidence intervals (CI) of results are reported for MOPA (HU n = 11, HEU n = 9) ; the serotype-specific IgG geometric mean concentration (GMC) (HU n = 11, HEU n = 8) for all PCV13 serotypes (1, 3, 4, 5, 6 A, 6B, 7F, 9V, 14, 18C, 19A, 19F, and 23F) are reported, less than 8 was reported as no response.

Figure Legends

Figure 1. Monocyte phagosomal functional capacity in HEU new borns and HU controls. The proportion of CD14+ cells that performed **a)** phagosomal superoxide burst activity, **b)** phagosomal bulk proteolytic activity, **c)** and that were associated with beads, **d)** the phagosomal superoxide burst activity index and **e)** the phagosomal bulk proteolytic activity index. The readout for the assay are reported as the median fluorescent intensity of the reporter fluorochrome at 60mins:10mins and 240mins:10mins for oxidative burst and bulk proteolysis, respectively. The activity index was calculated using a ratio of the reporter fluorochrome over the the calibration fluorochrome. Only individuals with an uptake of greater than ≥30% were used in the phagosomal analysis. Data are presented as medians [IQR] and analysed using Mann Whitney U test (HU, n=16; HEU, n=12).

Figure 2: Characterisation of B cell immune profiles in HEU and HU new borns

Cord blood was stained with the following fluorochrome-conjugated antibodies, anti-CD19 APC, anti-CD10 PE-Cy7, anti-CD21-FITC and anti-CD27 APC-CY7. Singlets were defined using FSC-A vs. FSC-H parameters and lymphocytes were gated using SSC-A and FSC-A. B cells were then gated using CD19 against SSC-A. **a)** The proportion of B cell subsets were clasified using CD10, CD21 and CD27 as follows**:** $CD10^{-}CD21^{+}CD27^{-}$ (naive), $CD10^{-}CD21^{-}CD27^{+}$ (resting memory), $CD10^{-}CD21^{+}CD27^{+}$ (activated memory), $CD10^{-}CD21^{-}CD27^{-}$ (tissue-like memory) and **c)** $CD10^{+}CD27^{-}$ (immature transitional).

b) Expression of CD95e450, FcLR4 PE and PD-1 APC (exhausted and activatory inhibited B-cells) were gated as a proportion of CD19+ cells.

Data are presented as medians [IQR] and analysed using Mann Whitney U test (HU n=42, HEU n=18 B cells and HU, n=41; HEU, n=24 T cells.).

Figure 3. Characterisation of T cell subsets in HEU and HU new borns. Whole cord blood was stained with the following fluorochrome-conjugated antibodies, anti-CD3 APCCY7, anti-CD4 Pacific Blue, anti-CD8-FITC, anti-CCR7 APC and anti-CD45RA PECY7 wereused to identify T cell subsets. Singlets were defined using FSC-A vs. FSC-H parameters and lymphocytes were gated using SSC-A and FSC-A. T cells were then gated using CD3 against SSC-A, then a CD4 versus CD8 plot was used to separate the two main T cell subsets A second panel of fluorochrome-conjugated antibodies, anti-CD3 APCCY7, anti-CD4 Pacific Blue, anti-CD8-PECY7 and CD57 FITC, PD1-PE were used to measure T cell senescence and exhaustion. (HU, n =36; HEU, n =25).

a)$CD4^+$ and **b**)$CD8^+$ T cell subsets were clasified using CCR7 and CD45RA as follows CCR7-CD45RA- (effector memory), $CCR7^+$CD45RA- (central memory), $CCR7^+CD45RA^+$ (naïve) and $CCR7^-$ $CD45RA^+$(terminally-differentiated). **c)** $CD4^+$ and $CD8^+$ T cell subsets were clasified using CD57 (senescent) and PD-1 (exhausted) expression, **d)** Isolated cord blood mononuclear cells were incubated with PHA or PPD for 18 hours and IFN-γ producing cells were detected on a 96-well microtitre ELISpot plate. The frequency of SFCs/million cord blood mononuclear cells are plotted for all subjects. (HU, n =35; HEU, n =21) Data analysed using Fisher's exact test. Error bars depict medians 95%CI.

Figure 4. Infant and maternal antibody responses. Preceding and following Penta-DTwPHibHepB vaccination we measured vaccine titers using an ELISA to **a**) anti-Hib IgG in infant serum at 5-7 (HU, n=50; HEU n=39), 14-15 (HU, n=22; HEU, n=27) and 18-23 (HU, n=25; HEU, n=19) weeks; and **b**) maternal anti-*Hib* IgG **c**) maternal anti-TT IgG at one timepoint in HIV- uninfected (n=61) and HIV-infected (n=43). Blue circles are controls and red are HEU infants or HIV-infected mothers. Green dotted horizontal line represents cut-off for protective titers. Data are presented as mean(95%CI) and analysed using Mann

Whitney U test. Minimum putative protective titres are 0.15ug/mL (passive) and 1.0ug/mL (acquired) for *Hib* [50], and 0.01IU/mL for TT and DT.

Figure 5: Infant exposure to immune modulating viruses HCMV and HIV

a) Detection of Gag-specific T-cells by T-cell ELISPOT assay in HU and HEU infants, and ART naïve/experienced HIV-infected adults . Isolated PBMCs were incubated with 15-mer Gag peptide pool, PHA as a positive control or RPMI media as a negative control. IFN-γ producing cells were detected on a 96-well microtitre ELISpot plate. **b)** The frequency of SFCs/million PBMCs are plotted for all subjects. Data analysed using Fisher's exact test (HU, n =22; HEU, n=34; HIV+ART+, n=17; HIV+ART-, n=8).

c) Plasma anti-CMV IgG was measured in infants between 5-15weeks of age and assigned an arbitrary titer. The proportion of **d)** HU and HEU infants and **e)** HIV-infected and uninfected mothers with RT-PCR detected CMV DNA in their oropharangeal throat swab and breast milk respectively, (HIV- n=23, HIV+ n=35). The proportion of **f)** HU and HEU infants who were seropositive for anti-EBV IgG (HU n=57, HEU n=42) and **g)** mothers who had detectable EBNA4 gene by RT-PCR, (HIV- n=23, HIV+ n=35). **IgG** data were analysed using Mann-Whitney U test reported as medians [IQR] and PCR data using a Fisher's exact test reporting effective size as a relative risk. Blue circles are HU controls and red circles are HEU. Data are presented as means [SD].

Supplementary Figures

Supplementary Figure 1: Gating strategy to detect monocyte phagosomal functional capacity at birth. Singlets were defined using FSC-A vs. FSC-H parameters and lymphocytes were gated using SSC-A and CD14 PE-CY7. Then FSC-A vs. AF405 to gate cells with beads. The readout for the assay are reported as the median fluorescent intensity of the reporter fluorochrome at 60mins:10mins and 240mins:10mins for oxidative burst and bulk proteolysis, respectively. The activity index was calculated using a ratio of the reporter fluorochrome over the the calibration fluorochrome. Only individuals with an uptake of greater than ≥30% were used in the phagosomal analysis. Data are reported as median[95%CI].

Supplementary figure 2: Characterisation of B cell and T cell subsets in HEU and HU infants

Using peripheral blood collected from the longitudinal infant cohort aged 5-9 weeks, whole blood was stained with the following fluorochrome-conjugated antibodies, anti-CD19 APC, anti-CD10 PE-Cy7, anti-CD21-FITC and anti-CD27 PE. Singlets were defined using FSC-A vs. FSC-H parameters and lymphocytes were gated using SSC-A and FSC-A. B cells were then gated using CD19 against SSC-A. **a)** The proportion of B cell subsets were clasified using CD10, CD21 and CD27 as follows**:** $CD10^{-}CD21^{+}CD27^{-}$ (naive), $CD10^{-}CD21^{-}CD27^{+}$ (resting memory), $CD10^{-}CD21^{+}CD27^{+}$ (activated memory), $CD10^{-}CD21^{-}CD27^{-}$ (tissue-like memory) and **c)** $CD10^{+}CD27^{-}$ (immature transitional).

The proportion of T cells were measured with the following fluorochrome-conjugated antibodies, anti-CD3 APCH7, anti-CD4 Pacific Blue, anti-CD8-FITC, anti-CCR7 APC and anti-CD45RA PE. Singlets were defined using FSC-A vs. FSC-H parameters and lymphocytes were gated using SSC-A and FSC-A. T cells were then gated using CD3 against SSC-A, then a CD4 versus CD8 plot was used to separate the two main T cell subsets. **b)**$CD4^{+}$ and **c**) $CD8^{+}$ T cell subsets were clasified using CCR7 and CD45RA as follows CCR7-CD45RA- (effector memory), $CCR7^{+}$CD45RA- (central memory), $CCR7^{+}CD45RA^{+}$ (naïve) and $CCR7^{-}$

CD45RA^{+}(terminally-differentiated). Data are presented as medians [IQR] and analysed using Mann Whitney U test (HU n=42, HEU n=31).

d) IFN-γ producing cells were measured using a T-cell ELISPOT assay in HU and HEU infants. Isolated PBMCs were incubated with either PPD, TT, Hb or PHA as a positive control or RPMI media as a negative control for 18 hours. IFN-γ producing cells were detected on a 96-well microtitre ELISpot plate. The frequency of SFCs/million PBMCs are plotted for all subjects. Data analysed using Fisher's exact test (HU, n =22; HEU, n=34), median[95%CI) reported.

Supplementary Figure 3: Gating strategy to characterise B cells from infant blood. a) Blood was stained with the following fluorochrome-conjugated antibodies, anti-CD19 APC, anti-CD10 PE-Cy7, anti-CD21-FITC and anti-CD27 APC-CY7. Singlets were defined using FSC-A vs. FSC-H parameters and lymphocytes were gated using SSC-A and FSC-A. B cells were then gated using CD19 against SSC-A. The following populations were determined: CD10^{-}CD21^{+}CD27^{-} (naive), CD10^{-}CD21^{-}CD27^{+} (resting memory), CD10^{-} CD21^{+}CD27^{+} (activated memory), CD10^{-}CD21^{-}CD27^{-} (tissue-like memory) and CD10^{+}CD27^{-} (immature transitional). **b)** Blood was stained with CD19 PERCP, anti-CD10 PE-Cy7, anti-CD21-FITC and anti-CD27 APCCY7, FcRL4 PE, CD95e450 and CD27 APCCY7 to determine B cells expressing inhibitory markers. **M**edian[95%CI) reported.

Supplementary Figure 4: Gating strategy to characterise B cells from cord blood. a) Blood was stained with the following fluorochrome-conjugated antibodies, anti-CD19 APC, anti-CD10 PE-Cy7, anti-CD21-FITC and anti-CD27 PE. Singlets were defined using FSC-A vs. FSC-H parameters and lymphocytes were gated using SSC-A and FSC-A. B cells were then gated using CD19 against SSC-A. The following populations were determined: CD10^{-}CD21^{+}CD27^{-} (naive), CD10^{-}CD21^{-}CD27^{+} (resting memory), CD10^{-} CD21^{+}CD27^{+} (activated memory), CD10^{-}CD21^{-}CD27^{-} (tissue-like memory) and CD10^{+}CD27^{-} (immature transitional). **b)** Blood was stained with CD19 PERCP, anti-CD10 PE-Cy7, anti-CD21-FITC and anti-CD27

APCCY7, FcRL4 PE, CD95e450 and CD27 APCCY7 to determine B cells expressing inhibitory markers. Median[95%CI) reported.

Supplementary Figure 5: Gating strategy to characterise T cell subsets. a) Whole blood was stained with the following fluorochrome-conjugated antibodies, anti-CD3 APCH7, anti-CD4 Pacific Blue, anti-CD8-FITC, anti-CCR7 APC and anti-CD45RA PE. **b)** Cord blood was stained with the following fluorochrome-conjugated antibodies, anti-CD3 APCY7, anti-CD4 Pacific Blue, anti-CD8-PECY7, anti-CCR7 APC and anti-CD45RA PECY5, PD-1 PE and CD57 FITC.

Singlets were defined using FSC-A vs. FSC-H parameters and lymphocytes were gated using SSC-A and FSC-A. T cells were then gated using CD3 against SSC-A, then a CD4 versus CD8 plot was used to separate the two main T cell subsets. FMO were used to determine gating. $CD4^+$ and $CD8^+$ T cell subsets were clasified using CCR7 and CD45RA as follows CCR7-CD45RA- (effector memory), $CCR7^+$CD45RA- (central memory), $CCR7^+CD45RA^+$ (naïve) and $CCR7^-CD45RA^+$(terminally-differentiated). Median[95%CI) reported.

Supplementary Figure 6: Infant and maternal antibody responses. Preceding and following Penta-DTwPHibHepB vaccination we measured vaccine titers using an ELISA to **a**) anti-TT IgG and **b**) anti-DT IgG in infants at 5-7 (HU, n=50; HEU n=39), 14-15 (HU, n=22; HEU, n=27) and 18-23 (HU, n=25; HEU, n=19) weeks. HIV- uninfected (n=61) and HIV-infected (n=43) maternal titres were measured for **c**) anti-DT IgG when infants were aged 5-7 weeks old. Blue circles are controls and red are HEU infants or HIV-infected mothers. Green dotted horizontal line represents cut-off for protective titers. Percentage of seropositivity is depicted inbar charts. Data are presented as medians and analysed using Mann Whitney U test. Minimum putative protective titres are 0.15ug/mL (passive) and 1.0ug/mL (acquired) for *Hib* [50], and 0.01IU/mL for TT and DT. Median[95%CI) reported.

Supplementary Figure 7: IFN-γ producing cells to HIV protein GAG at birth

A 15-mer GAG peptide pool was used to stimulate isolated cord blood mononuclear cells from cord blood in an 18hour T cell EliSpot assay. IFN-γ producing cells were detected on a 96-well microtitre ELISpot plate. **a)** The frequency of GAG SFCs/million cord blood mononuclear cells are plotted for all subjects. Data analysed using Fisher's exact test (HU, n =35; HEU, n=23). Median[95%CI) reported.

Supplementary Figure 8: Infant exposure to immune modulating viruses HCMV and EBV. HCMV and EBV viral DNA was measured by RT-PCR and anti-EBV IgG using an ELISA: **a)** Infant oropharangeal throat swab CMV DNA RT-PCR, (HU, n =19; HEU n=33), **b)** infant plasma anti-EBV IgG and **c**) HIV-infected and uninfected mothers with EBV RT-PCR detected in breast milk, (HIV- n=24, HIV+ n=34). Data analysed using Fisher's exact test and effective size reported as a relative risk. Median[95%CI) reported.

Supplementary Tables

Supplementary Table 1. Fluorochromes

Supplementary Table 2. Fluorescent antibody panels

Figure 1

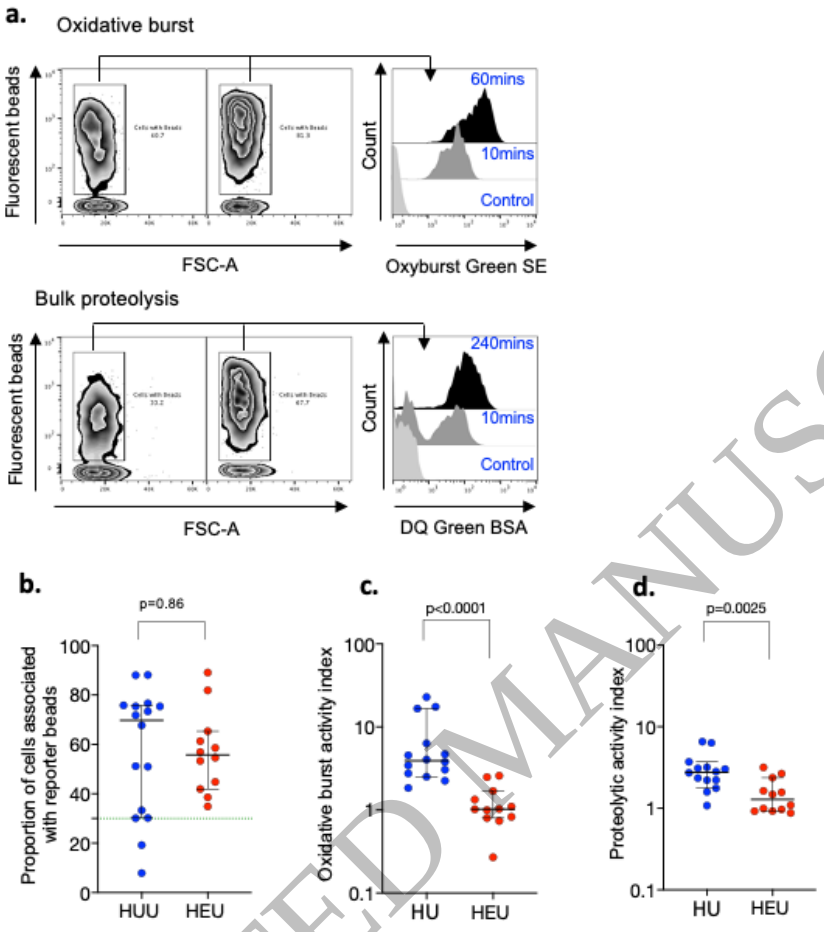

158x229 mm (5.7 x DPI)

Figure 2

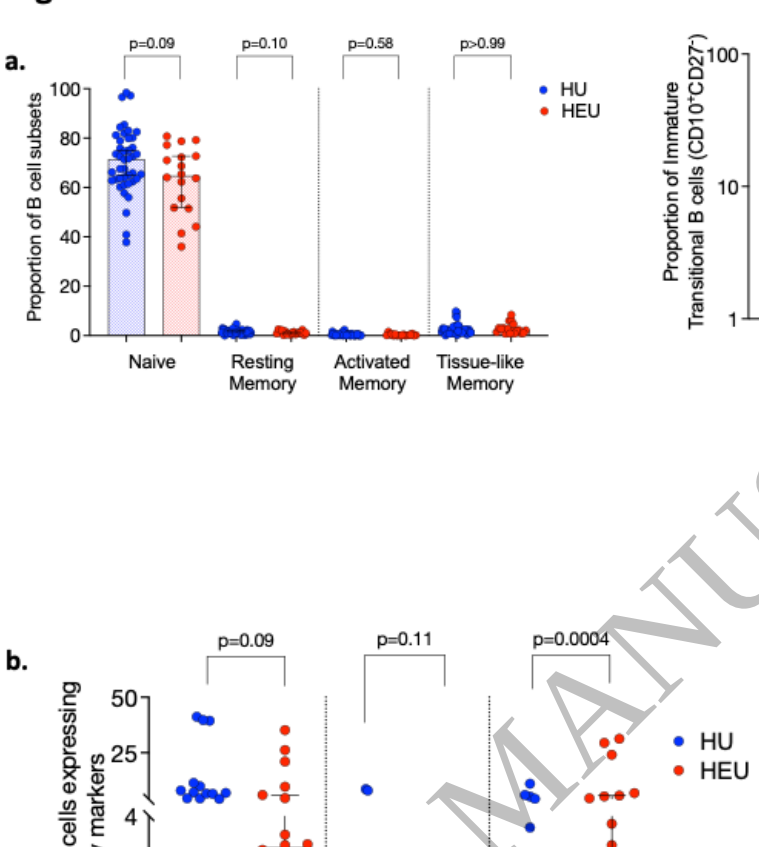

158x229 mm (5.7 x DPI)

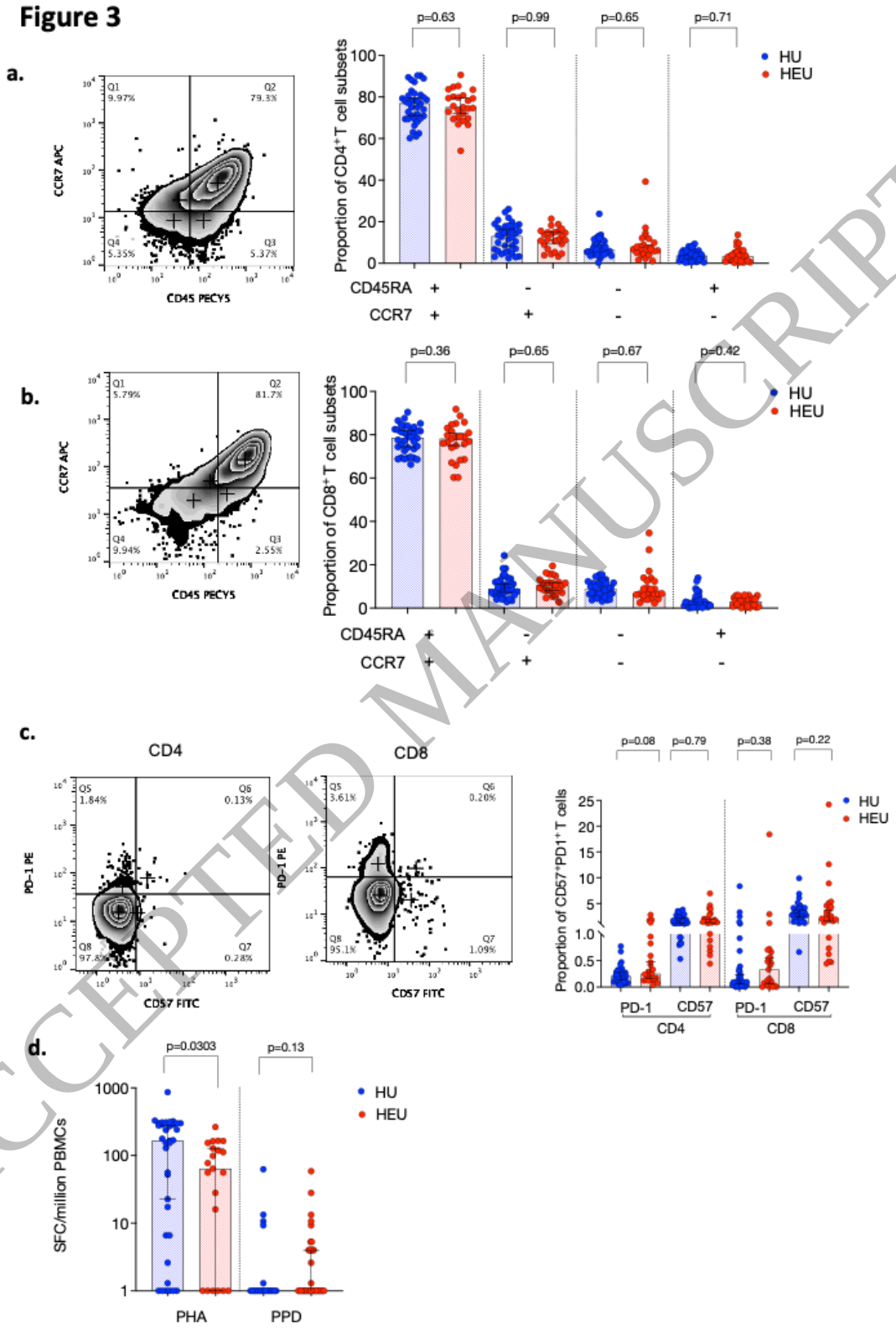

158x229 mm (5.7 x DPI)

Figure 4

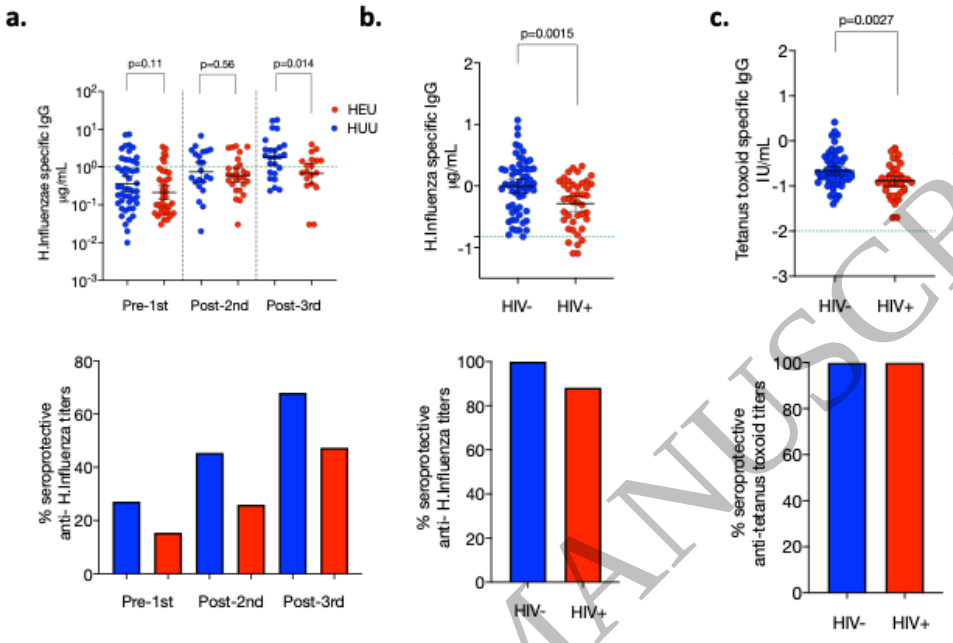

158x229 mm (5.7 x DPI)

Figure 5

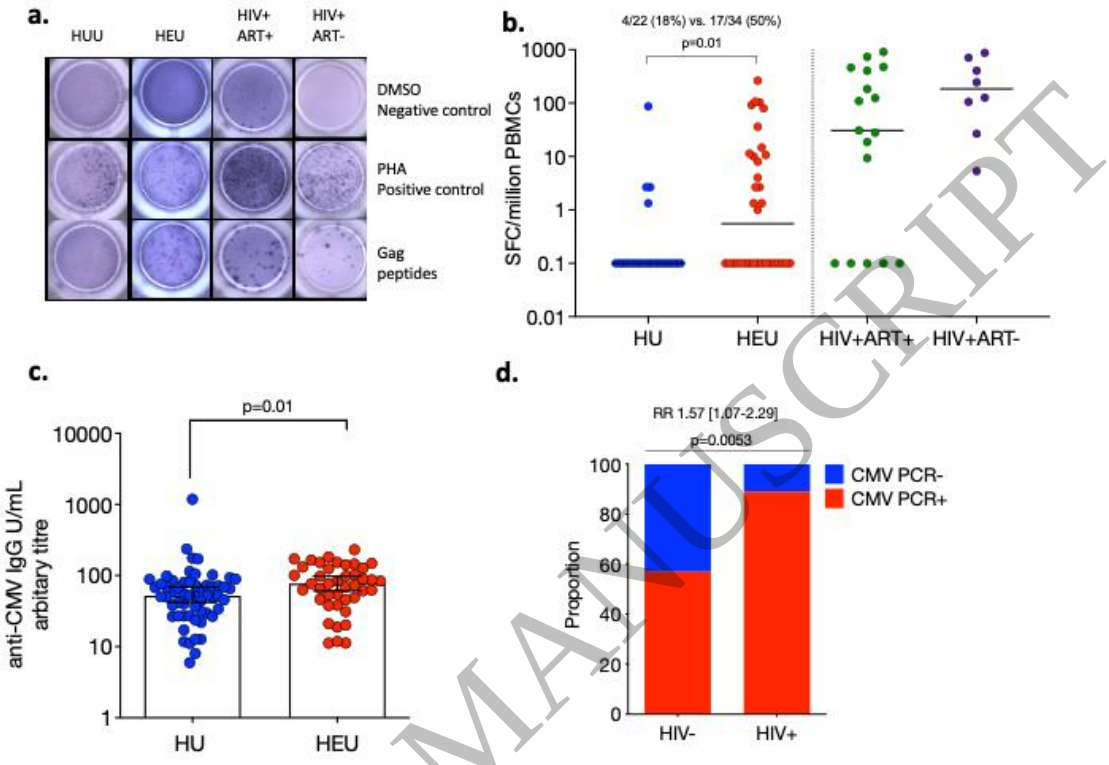

158x229 mm (5.7 x DPI)